

# One-step synthesis of fluorescent hydroxyls-coated carbon dots with hydrothermal reaction and its application to optical sensing of metal ions

LIU LiQin<sup>1</sup>, LI YuanFang<sup>1</sup>, ZHAN Lei<sup>2</sup>, LIU Yue<sup>1</sup> & HUANG ChengZhi<sup>1, 2\*</sup>

<sup>1</sup>Education Ministry Key Laboratory on Luminescence and Real-Time Analysis; College of Chemistry and Chemical Engineering, Southwest University, Chongqing 400715, China

<sup>2</sup>College of Pharmaceutical Sciences, Southwest University, Chongqing 400715, China

Received April 29, 2011; accepted June 2, 2011

Carbon dots (CDs) with average diameter of  $3.1 \pm 0.5$  nm were facilely synthesized with candle soot through hydrothermal reaction in sodium hydroxide aqueous solution. The as-prepared CDs were covered with a lot of hydroxyls, possessed properties of good water-solubility, anti-photobleaching, salt tolerance, and low cytotoxicity, and had a fluorescence quantum yield (QY) of about 5.5%. The fluorescence of the hydroxyls-coated CDs could be selectively quenched by metal ions such as  $\text{Cr}^{3+}$ ,  $\text{Al}^{3+}$  and  $\text{Fe}^{3+}$ , which is because these metals can easily combine with the hydroxyl groups on the surface of CDs and induce aggregation of hydroxyls-coated CDs. Experiments showed that the quenching of  $\text{Cr}^{3+}$  had a Stern-Volmer constant of  $1.03 \times 10^7 \text{ M}^{-1}$  with a liner range of 1.0–25.0  $\mu\text{M}$  and detection limit of 60 nM ( $3\sigma$ ).

**carbon dots, fluorescence, quantum yield, cytotoxicity, metal ions**

## 1 Introduction

In recent years, fluorescent semiconductor quantum dots (QDs) have been found wide applications in bioimaging and biomedicine due to their unique fluorescence properties and small size characteristics [1–5]. However, some researchers proposed that the heavy metals in QDs, such as cadmium, have some extent of cytotoxicity, which greatly confines their practical applications [6–8]. In such case, developing new fluorescent nanomaterials with low toxicity and good fluorescent features is an alternative strategy. Carbon dots (CDs), namely fluorescent carbon nanoparticles with size below 10 nm, have low toxicity and extraordinary optoelectrical properties [9–12] and these properties make them become excellent candidates for potential applications. At present, CDs have got preliminary applications in bioimag-

ing [13–15], biochemical analysis [16, 17], photocatalysis and white light-emitting devices [18, 19].

In 2004, Xu *et al.* first discovered CDs when separating and purifying single-walled carbon nanotubes (SWCNTs) derived from arc-discharge soot by electrophoresis [20], which was exciting but the fluorescence emissions of such CDs were not ideal. In 2006, Sun *et al.* proposed a new route to produce CDs with relatively good fluorescence emission, and firstly named the fluorescent carbon nanoparticles with the size below 10 nm as CDs [9]. These CDs were prepared via laser ablation of carbon target, then treated with nitric acid solution and further surface modification. Thereafter, a number of methods were established to synthesize CDs. For instance, soot-based carbon sources were refluxed in nitric acid and then separated to obtain CDs [21–24], while citric acid served as carbon source with a compensating organic ammonium providing the covalently attached surface modifier to produce carbogenic dots [25, 26]. Graphite provided the source of carbon by

\*Corresponding author (email: chengzhi@swu.edu.cn)

electrochemical soaking to generate CDs [11, 27]. However, the quantum yield (QY) of CDs obtained through the above methods besides Sun's was low, usually below 3.0%. Recently, Wang *et al.* synthesized a new type of fluorescent CDs with the QY of about 53% [28, 29], which, however, were oil soluble, greatly restraining their applications in biochemical analysis. Up to now, most of the fluorescent QY about water soluble CDs are still below 20%, and the preparation of water soluble CDs is usually multistep [9, 30], complicated and time-consuming.

Of these methods, the soot-based ways are simple and economical, but numerous carboxyls covered on the surface of CDs through refluxing with nitric acid greatly confine the QY. In order to improve the QY, soot-based routes usually need complicated separation or further modification [21, 22, 24]. Herein, we reported a facile route to synthesize fluorescent CDs which have great amounts of hydroxyls without complicated separation and further modification of the surface (Scheme 1). The QY can reach 5.5%, which is higher than those CDs reported from refs [11, 20–27, 31, 32]. We suppose that hydroxyls have strong electron donated ability, which benefit the fluorescence emission, while carboxyls have strong electron drawing ability with the opposite effect, thus the fluorescence properties of hydroxyls-coated CDs are better than those carboxyls-coated [33]. In addition, the fluorescence signals of the as-prepared CDs are stable for more than 6 months at 4 °C.

## 2 Experimental

### 2.1 Apparatus and materials

Polytetrafluoroethylene reaction kettle and electroheat blasting baking oven (CS101-IEBN) were used for the synthesis of CDs. Fluorescence emission and absorption spectra were recorded with an F-2500 fluorescent spectrophotometer and a UV-3010 spectrophotometer (Hitachi Ltd., Tokyo, Japan) respectively. A transmission electron microscope (TEM) (JEOL, Tokyo, Japan) and Zetasizer Nano ZS (Malvern, Herrenberg, Germany) were required to characterize the size of CDs. Infrared spectrum was obtained by a Perkin Elmer Spectrum GX Fourier Transform Infrared (FT-IR) Spectrometer (MA, USA) in KBr wafer. Fluorescence lifetimes were measured with a FL-TCSPC fluorescent spectrophotometer (Horiba Jobin Yvon Inc, France).

Candle soot was collected by putting a clean glass sheet on the top of the flame of candles (candles were purchased

from the local supermarket). Sodium hydrate (NaOH, 99%) and hydrogen chloride (HCl, 37%) were purchased from Chuandong Chemical Group Co., Ltd. Trichloride ferric was purchased from Chongqing Mao Industry Chemical Reagent Co., Ltd. Aluminum sulfate was purchased from Chengdu Jinshan Chemical Reagent Co., Ltd. Britton-Robinson buffer solution was used to control the acidity. Sodium chloride (5 M) was employed to adjust the ion strength of the solutions. Deionized water (18.2 MΩ cm) was used throughout the experiments. Stock solution of CDs (196 µg/mL) was prepared in water and stocked at 4 °C.

### 2.2 Synthesis and purification of CDs

25 mg candle soot collected as above was dispersed in 40 mL of 25 M NaOH solution by sonication for 30 min using a cup-horn sonicator (KH-100B). The mixture was transferred to a 100 mL polytetrafluoroethylene reaction kettle, which was in an electroheat blasting baking oven with 200 °C for 12 h. After that, the product cooled to ambient temperature naturally, and a brown-yellow supernatant was obtained by centrifuging at 12000 g for 15 min to get rid of the dark insoluble substances. Then, they were adjusted to near neutral with HCl (37 wt%) and filtered with a 0.22 µm filter membrane to remove the larger product, and then dialyzed against deionized water through a dialyzer with molecular weight cutoff 3500 Da for 2 days.

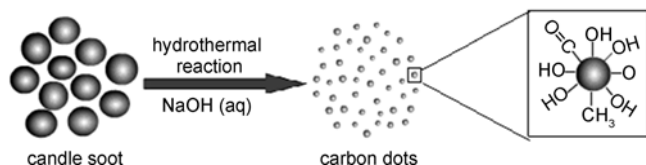
## 3 Results and discussion

### 3.1 Synthesis and characterization of CDs

By testing the quality and the QY of CDs at different reactive temperature and time, we optimized the best condition for the synthesis of CDs, that is, reflux for 12 h at 200 °C (Figure S1, S2, and Table S1).

The transmission electron microscopic (TEM) image of CDs in Figure 1 showed that the nanoparticles were mono-dispersed and uniform with spherical shape, and the size was  $3.1 \pm 0.5$  nm in diameter. Dynamic light scattering (DLS) measurements showed that the CDs were also narrowly distributed (Figure S4). In addition, zeta potential result showed that the CDs were negatively charged (Figure S5), resulting from the ionized hydroxyls in weak alkaline conditions. The formation of hydroxyls was owing to the corrosion of the surface of carbon particles by sodium hydrate [34], and therefore the CDs can be easily dispersed in water medium.

Fourier Transform Infrared (FT-IR) measurements showed that there were typical peaks around  $3421\text{ cm}^{-1}$  and  $1401\text{ cm}^{-1}$  (Figure 2), which were ascribed to the stretching vibrations and in-plane bending vibration of  $\text{-OH}$ , respectively [35]. The dull and intense band of  $3421\text{ cm}^{-1}$  indicated the existence of hydrogen bonds, and that at  $1642\text{ cm}^{-1}$  manifested the existence of carbonyl ( $\text{C=O}$ ). The band at



**Scheme 1** Preparation procedure of fluorescent hydroxyls-coated CDs.

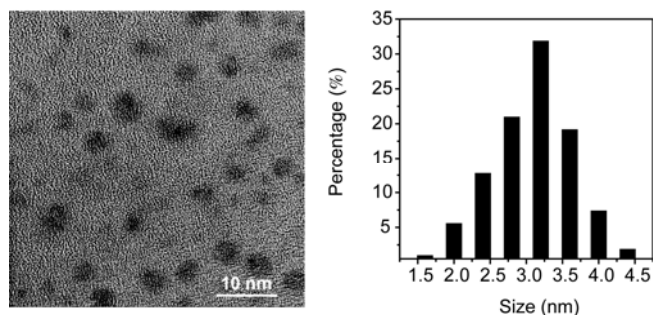


**Figure 1** TEM image of CDs (left) and the size distribution of CDs (right).

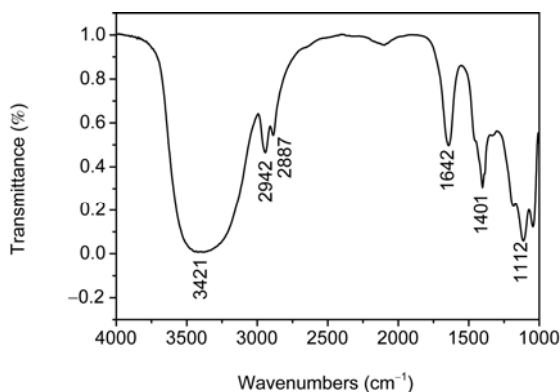


**Figure 2** FT-IR spectrum of the as-prepared CDs powder.

1112 cm<sup>-1</sup> should be ascribed to the stretching vibrations of C–O, while that at 2943 cm<sup>-1</sup> and 2887 cm<sup>-1</sup> corresponded to the stretching vibration of C–H in the group of –CH<sub>3</sub> or –CH<sub>2</sub>, indicating that the combustion of diolefine in candle soot was not greatly completed.

### 3.2 Absorption and emission features of CDs

Figure 3 is the absorption and fluorescence spectra of CDs in aqueous solution in UV-vis range. The CDs have a largely featureless profile absorption, which is consistent with indirect bandgap semiconductor nanoparticles, thus the CDs belong to indirect bandgap semiconductor materials in some extent. The CDs also have the narrow and symmetry excitation and emission features, characterized at 310 nm and 450 nm, respectively. As noticed, the large Stoke's shift is beneficial for the distinction of the target from the background signal in imaging. Additionally, the emission was dependent on excitation energy, that is the emission got shifted to longer wavelengths as the excitation wavelength got increased, (Figure S6), which may reflect the CDs have different sizes or different light-emitting sites.

The fluorescence emission of CDs depends on the pH values of the medium, and gets stable only in conditions of pH ≥ 7 (Figure S7). Moreover, this pH-dependence of the fluorescence emission is reversible. In acid condition, it is very easy for the adjacent hydroxyls on the surfaces of CDs to form hydrogen bonds, inducing aggregation of CDs and

as a result, the fluorescence emission of CDs is quenched. In alkaline condition, however, the CDs are monodispersed and the fluorescence emission remains stable. In addition, the fluorescence intensity of CDs changes hardly at 0–2.0 M NaCl aqueous solution (Figure S8), indicating that the CDs have high salt tolerance. The CDs also show considerable photostability within 30 min under continuous excitation (Figure S9), suggesting that CDs have the potential as candidates for targeted tracing and cells imaging.

Besides, the CDs also show low cytotoxicity as displayed by the results of the CKK-8 assays of cell viability (Figure 4) and the details in supporting information. Such low cytotoxicity of CDs might be related to the usage of the raw materials, which are chemically inert, non-toxic, and do not release any toxic species even in a harsh environment. Thus, the low cytotoxicity would make the CDs suitable for *in vivo* labeling and imaging.

### 3.3 The quantum yield and luminescence mechanism

The fluorescence QY of hydroxyls-coated CDs is about

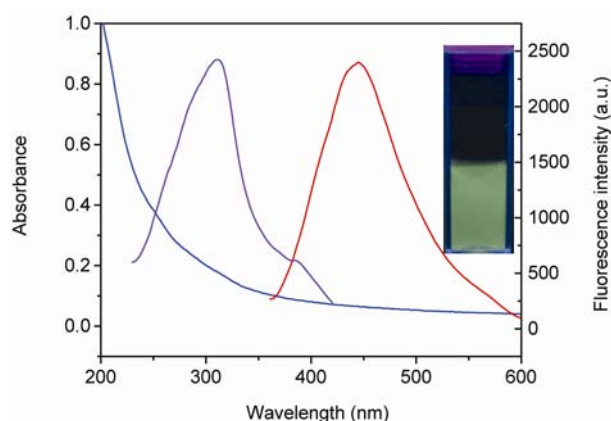


**Figure 3** UV-vis absorption (blue line), fluorescence excitation (violet line) and emission (red line) spectra of CDs in aqueous solution. Inset: photo of CDs in aqueous solution caught when illuminated with a 365 nm UV lamp.

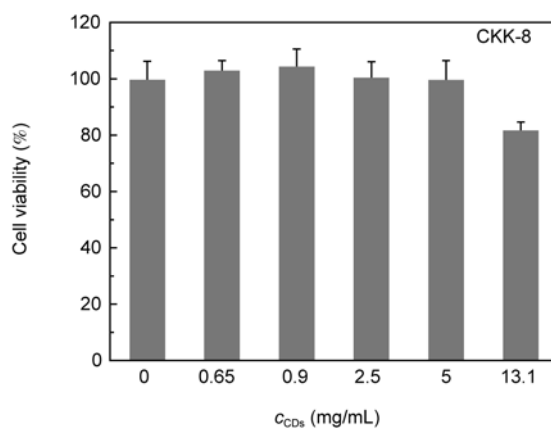
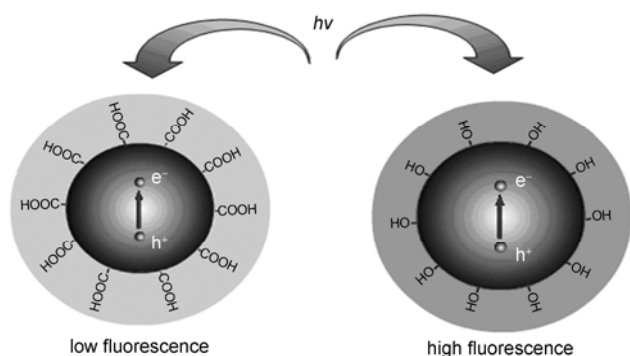


**Figure 4** Cytotoxicity of CDs for HeLa cell studied by CKK-8. All data were average of three experiments.

5.5% with quinine sulfate as a standard reference (Figure S3, Table S1). This value is substantially higher than that of the CDs obtained by refluxing with nitric acid followed by complicated separation or modification procedures [21, 22, 24], and comparable with the previously reported value for fluorescent carbon nanoparticles [31, 36, 37].

Currently, the luminescence mechanism of CDs is still not clear. Most of the investigations showed that the surface passivation process could highly improve the QY of CDs [9, 28–32, 37]. This requirement was also shared by silicon nanocrystals and metal QDs, for which a widely accepted mechanism for luminescence was the radiative recombination of excitons [38–41]. In our experiment, the raw materials, namely candle soot and sodium hydrate, have no fluorescence property, thus the production of fluorophore is impossible in the condition of high temperature, high pressure and the strong alkali corrosion. The size of CDs reported here is lower than 10 nm, which have quantum size effect and quantum confinement effect that would make the continuous energy band become discrete at the molecular level [42–44]. Additionally, the fluorescence lifetime of CDs is about 9.5 ns, such a short lifetime indicates the radiative recombination nature of excitations (Figure S10) [37]. Based on the above aspects, we believe that the luminescence mechanism of our obtained CDs is the radiative recombination nature of excitations other than common organic fluorescence molecules.

The fluorescence emission of hydroxyls-coated CDs is better than those carboxyls-coated CDs when taking soot as the carbon source. As shown in Scheme 2, when hydroxyls or carboxyls are bonded onto the surface of CDs directly (namely without spacer), radiative recombination between electrons and holes takes place under the illumination of excitation light, and thus fluorescence emission occurs. We suppose that the surface carboxyls with strong electron drawing ability adsorb some emission signals, which decreases the fluorescence emission, while hydroxyls with strong electron donated ability would be a great benefit to fluorescence emission [33]. Thus hydroxyls-coated CDs have better fluorescence emission ability than those carboxyls-coated.



**Scheme 2** The schematic illustrates fluorescence emission of hydroxyls-coated CDs is better than that of carboxyls-coated CDs. (e<sup>-</sup>: electron, h<sup>+</sup>: hole)

### 3.4 The application of CDs in metal ions detection

We further investigated the interaction between hydroxyls-coated CDs and metal ions. Theoretically, metal ions with the very low solubility product constant ( $K_{sp}$ ) of metal hydroxides are easy to combine with hydroxyls on the surface of CDs, and made the CDs aggregate, causing fluorescence quenching. Figure 5 shows that  $Hg^{2+}$ ,  $Cr^{3+}$ ,  $Al^{3+}$ , and  $Fe^{3+}$  can easily quench the fluorescence effect, which is possibly because these metal ions have lower  $K_{sp}$  of metal hydroxides (the  $K_{sp}$  of  $Hg(OH)_2$ ,  $Cr(OH)_3$ ,  $Al(OH)_3$  and  $Fe(OH)_3$  are  $3.6 \times 10^{-26}$ ,  $6.3 \times 10^{-31}$ ,  $1.3 \times 10^{-33}$ ,  $4.0 \times 10^{-38}$ , respectively), while the other metal ions with relatively high  $K_{sp}$  have weak quenching effect.

The above results suggest that hydroxyls-coated CDs have a potential application in biocompatible nanosensors for measuring  $Cr^{3+}$ ,  $Al^{3+}$  and  $Fe^{3+}$  in human body fluids (the content of  $Hg^{2+}$  is extremely low). For instance, if we need to detect  $Cr^{3+}$ , we can mask  $Al^{3+}$ ,  $Fe^{3+}$  by adding fluorine ions. The other two metal ions can be detected in the similar way. Herein we have a detailed study for the detection of  $Cr^{3+}$ .

Under the optimum conditions, the CDs fluorescence intensity is quenched by  $Cr^{3+}$  with a linear range from 1 to 25  $\mu M$  with a detection limit of 60 nM ( $3\sigma$ ) (Figure 6). To further analyze the quenching mechanism, we measured the fluorescence lifetimes change of CDs before and after adding  $Cr^{3+}$ . As shown in Figure 7, the fluorescence lifetime has no variation, indicating that the quenching followed a static process [45, 46]. Stern-Volmer plots were almost linear (Figure 8), deriving a static Stern-Volmer constant ( $K_{sv}$ ) of  $1.03 \times 10^7 M^{-1}$  from the plots of  $F_0/F$ , which indicates the high quenching efficiency of  $Cr^{3+}$  to the CDs.

## 4 Conclusions

In summary, we developed a novel and convenient route to synthesize hydroxyls-coated CDs by one-step hydrothermal reaction. It was found that the hydroxyls-coated CDs had better fluorescence properties than carboxyls-coated CDs

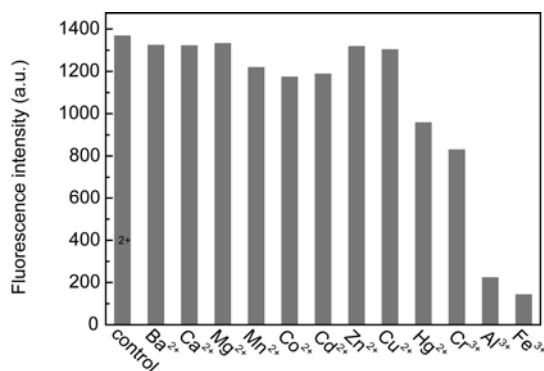


**Figure 5** Effect of metal ions on CDs fluorescence intensity. All concentration of metal ions is  $5.0 \times 10^{-6} M$ ,  $c_{CDs}$   $39.2 \mu g mL^{-1}$ , buffer (Tris-HCl) pH 5.38,  $\lambda_{ex}$  310 nm,  $\lambda_{em}$  450 nm.

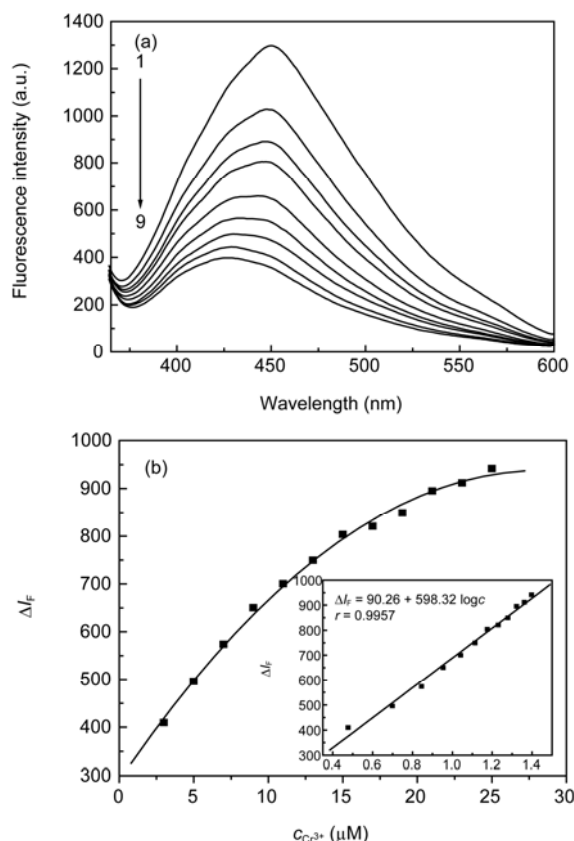


**Figure 6** (a) Fluorescence emission spectra of CDs in aqueous solution with different concentration of  $\text{Cr}^{3+}$ .  $c_{\text{Cr}^{3+}}$ : 0, 1, 2, 3, 5, 9, 13, 17, 21, 25  $\mu\text{M}$  (from 1 to 9).  $c_{\text{CDs}}$  39.2  $\mu\text{g/mL}$ , buffer (Tris-HCl) pH 5.38,  $\lambda_{\text{ex}}$  310 nm,  $\lambda_{\text{em}}$  450 nm; (b) the calibration curves for (a), the inset is logarithm fit for calibration curves.

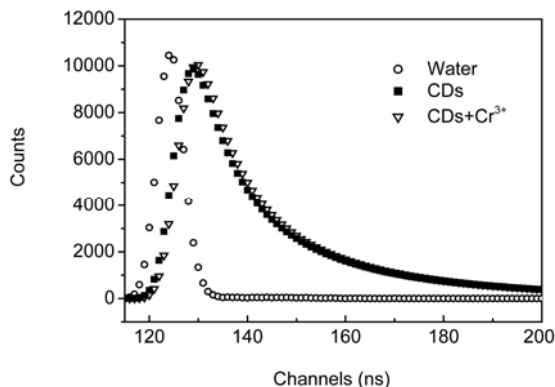


**Figure 7** Fluorescence decay curves of pure CDs and CDs after their interaction with  $\text{Cr}^{3+}$ .

with good water-solubility, light stability, salt endurance, high fluorescent QY, and low cytotoxicity. These properties would make CDs have extensive applications in bioimaging, sensors, catalysis and other fields in the near future. At the same time, hydroxyls-coated CDs were applied to detecting metal ions with very low  $K_{\text{sp}}$  of metal hydroxides, which give a good result.

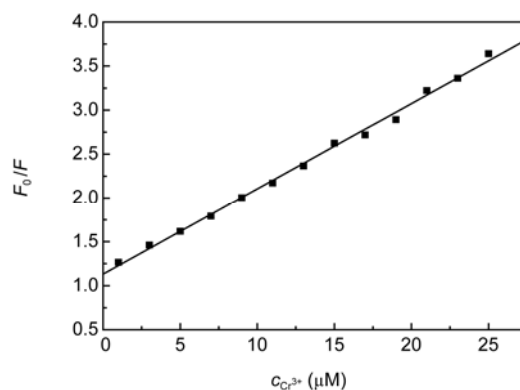


**Figure 8** Stern-Volmer plots of the fluorescence quenching of CDs in aqueous solution by  $\text{Cr}^{3+}$ .

This work was financially supported by the National Natural Science Foundation of China (21035005).

- Han M, Gao X, Su JZ, Nie S. Quantum-dot-tagged microbeads for multiplexed optical coding of biomolecules. *Nat Biotechnol*, 2001, 19: 631–635
- Jaiswal JK, Mattoussi H, Mauro JM, Simon SM. Long-term multiple color imaging of live cells using quantum dot bioconjugates. *Nat Biotechnol*, 2002, 21: 47–51
- Myung N, Ding Z, Bard AJ. Electrogenerated chemiluminescence of CdSe nanocrystals. *Nano Lett*, 2002, 2: 1315–1319
- Michalet X, Pinaud FF, Bentolila LA, Tsay JM, Doose S, Li JJ, Sundaresan G, Wu AM, Gambhir SS, Weiss S. Quantum dots for live cells, in vivo imaging, and diagnostics. *Science*, 2005, 307: 538–544
- Wang XX, Yang ZK, San Z, Pen X, Huang QM. Preparation of giant unilamellar CdTe quantum dot vesicles and their metabolic pathway in vivo. *Sci China Chem*, 2010, 53: 1718–1722
- Hardman R. A toxicologic review of quantum dots: toxicity depends on physicochemical and environmental factors. *Environ Health Perspect*, 2006, 114: 165–172
- Geys J, Nemmar A, Verbeken E, Smolders E, Rato M, Hoylaerts MF, Nemery B, Hoet PHM. Acute toxicity and prothrombotic effects of quantum dots: impact of surface charge. *Environ Health Perspect*, 2008, 116: 1607–1613
- Li HC, Luo WR, Tao Y, Wu Y, Lv XF, Zhou QF, Jiang JB. Effects of nanoscale quantum dots in male Chinese loaches (*Misgurnus anguillicaudatus*): Estrogenic interference action, toxicokinetics and oxidative stress. *Sci China Chem*, 2009, 52: 1683–1690
- Sun YP, Zhou B, Lin Y, Wang W, Fernando KAS, Pathak P, Meziani MJ, Harruff BA, Wang X, Wang H, Luo PG, Yang H, Kose ME, Chen B, Veca LM, Xie SY. Quantum-sized carbon dots for bright and colorful photoluminescence. *J Am Chem Soc*, 2006, 128: 7756–7757
- Cao L, Wang X, Meziani MJ, Lu F, Wang H, Luo PG, Lin Y, Harruff BA, Veca LM, Murray D, Xie SY, Sun Y-P. Carbon dots for multiphoton bioimaging. *J Am Chem Soc*, 2007, 129: 11318–11319
- Zhao QL, Zhang ZL, Huang BH, Peng J, Zhang M, Pang DW. Facile preparation of low cytotoxicity fluorescent carbon nanocrystals by electrooxidation of graphite. *Chem Commun*, 2008, 5116–5118
- Wang X, Cao L, Lu F, Meziani MJ, Li H, Qi G, Zhou B, Harruff BA, Kermarrec F, Sun YP. Photoinduced electron transfers with carbon dots. *Chem Commun*, 2009, 3774–3776
- Yang ST, Cao L, Luo PG, Lu F, Wang X, Wang H, Meziani MJ, Liu Y, Qi G, Sun YP. Carbon dots for optical imaging in vivo. *J Am Chem Soc*, 2009, 131: 11308–11309
- Yang ST, Wang X, Wang H, Lu F, Luo PG, Cao L, Meziani MJ, Liu JH, Liu Y, Chen M, Huang Y, Sun YP. Carbon dots as nontoxic and high-performance fluorescence imaging agents. *J Phys Chem C*, 2009,

- 113: 18110–18114
- 15 Li Q, Ohulchanskyy TY, Liu R, Koynov K, Wu D, Best A, Kumar R, Bonoiu A, Prasad PN. Photoluminescent carbon dots as biocompatible nanoprobe for targeting cancer cells *in vitro*. *J Phys Chem C*, 2010, 114: 2062–2068
- 16 Gonçalves H, Jorge PAS, Fernandes JRA, Silva JCGEd. Hg(II) sensing based on functionalized carbon dots obtained by direct laser ablation. *Sensor Actuat B-Chem*, 2010, 145: 702–707
- 17 Zhao HX, Liu LQ, Liu ZD, Wang Y, Zhao XJ, Huang CZ. Highly selective detection of phosphate in very complicated matrixes with an off an off-on fluorescent probe of europium-adjusted carbon dots. *Chem Commun*, 2011, 47: 2604–2606
- 18 Li H, He X, Kang Z, Huang H, Liu Y, Liu J, Lian S, Tsang CHA, Yang X, Lee ST. Water-soluble fluorescent carbon quantum dots and photocatalyst design. *Angew Chem Int Ed*, 2010, 49: 4430–4434
- 19 Wang F, Chen YH, Liu CY, Ma DG. White light-emitting devices based on carbon dots electroluminescence. *Chem Commun*, 2011, 47: 3502–3504
- 20 Xu X, Ray R, Gu Y, Ploehn HJ, Gearheart L, Raker K, Scrivens WA. Electrophoretic analysis and purification of fluorescent single-walled carbon nanotube fragments. *J Am Chem Soc*, 2004, 126: 12736–12737
- 21 Liu H, Ye T, Mao C. Fluorescent carbon nanoparticles derived from candle soot. *Angew Chem Int Ed*, 2007, 46: 6473–6475
- 22 Ray SC, Saha A, Jana NR, Sarkar R. Fluorescent carbon nanoparticles: synthesis, characterization, and bioimaging application. *J Phys Chem C*, 2009, 113: 18546–18551
- 23 Tian L, Ghosh D, Chen W, Pradhan S, Chang X, Chen S. Nanosized carbon particles from natural gas soot. *Chem Mater*, 2009, 21: 2803–2809
- 24 Mao XJ, Zheng HZ, Long YJ, Du J, Hao JY, Wang LL, Zhou DB. Study on the fluorescence characteristics of carbon dots. *Spectrochim Acta Part A*, 2010, 75: 553–557
- 25 Bourlinos AB, Stassinopoulos A, Anglos D, Zboril R, Georgakilas V, Giannelis EP. Photoluminescent carbogenic dots. *Chem Mater*, 2008, 20: 4539–4541
- 26 Bourlinos AB, Stassinopoulos A, Anglos D, Zboril R, Karakassides M, Giannelis EP. Surface functionalized carbogenic quantum dots. *Small*, 2008, 4: 455–458
- 27 Lu J, Yang JX, Wang J, Lim A, Wang S, Loh KP. One-pot synthesis of fluorescent carbon nanoribbons, nanoparticles, and graphene by the exfoliation of graphite in ionic liquids. *ACS Nano*, 2009, 3: 2367–2375
- 28 Wang F, Pang S, Wang L, Li Q, Kreiter M, Liu CY. One-step synthesis of highly luminescent carbon dots in noncoordinating solvents. *Chem Mater*, 2010, 22: 4528–4530
- 29 Wang F, Xie Z, Zhang H, Liu CY, Zhang YG. Highly luminescent organosilane-functionalized carbon dots. *Adv Funct Mater*, 2011, 21: 1027–1031
- 30 Liu R, Wu D, Liu S, Koynov K, Knoll W, Li Q. An aqueous route to multicolor photoluminescent carbon dots using silica spheres as carriers. *Angew Chem Int Ed*, 2009, 121: 4668–4671
- 31 Hu SL, Niu KY, Sun J, Yang J, Zhao NQ, Du XW. One-step synthesis of fluorescent carbon nanoparticles by laser irradiation. *J Mater Chem*, 2009, 19: 484–488
- 32 Peng H, Trivas-Sejdic J. Simple aqueous solution route to luminescent carbogenic dots from carbohydrates. *Chem Mater*, 2009, 21: 5563–5565
- 33 Xing QY, Pei WW, Xu RQ, Pei J. *Fundamental Organic Chemistry (3rd ed.)*. Beijing: Higher Education Press, 2005, 243–245
- 34 Pan H, Liu L, Guo ZX, Dai L, Zhang F, Zhu D, Czerw R, Carroll DL. Carbon nanotubols from mechanochemical reaction. *Nano Lett*, 2002, 3: 29–32
- 35 Iijima S. Helical microtubules of graphitic carbon. *Nature*, 1991, 354: 56–58
- 36 Zhou J, Booker C, Li R, Zhou X, Sham TK, Sun X, Ding Z. An electrochemical avenue to blue luminescent nanocrystals from multiwalled carbon nanotubes (MWCNTs). *J Am Chem Soc*, 2007, 129: 744–745
- 37 Zhu H, Wang X, Li Y, Wang Z, Yang F, Yang X. Microwave synthesis of fluorescent carbon nanoparticles with electrochemiluminescence properties. *Chem Commun*, 2009, 5118–5120
- 38 Wilson WL, Szajowski PF, Brus LE. Quantum confinement in size-selected, surface-oxidized siliconnanocrystals. *Science*, 1993, 262: 1242–1244
- 39 Li ZF, Ruckenstein E. Water-soluble poly(acrylic acid) grafted luminescent silicon nanoparticles and their use as fluorescent biological staining labels. *Nano Lett*, 2004, 4: 1463–1467
- 40 Holmes JD, Johnston KP, Doty RC, Korgel BA. Control of thickness and orientation of solution-grown silicon nanowires. *Science*, 2000, 287: 1471–1473
- 41 Myung N, Bae Y, Bard AJ. Effect of surface passivation on the electrogenerated chemiluminescence of CdSe/ZnSe nanocrystals. *Nano Lett*, 2003, 3: 1053–1055
- 42 Chestnoy N, Harris TD, Hull R, Brus LE. Luminescence and photophysics of cadmium sulfide semiconductor clusters: the nature of the emitting electronic state. *J Phys Chem C*, 1986, 90: 3393–3399
- 43 Henglein A. Small-particle research: Physicochemical properties of extremely small colloidal metal and semiconductor particles. *Chem Rev*, 1989, 89: 1861–1873
- 44 Halperin WP. Quantum size effects in metal particles. *Rev Mod Phys*, 1986, 58: 533–606
- 45 Zeng HL, Durocher G. Analysis of fluorescence quenching in some antioxidants from non-linear stern-volmer plots. *J Lumin*, 1995, 63: 75–84
- 46 Valero M, López-Cornejo MP, Costa SMB. Effect of the structure and concentration of cyclodextrins in the quenching process of naproxen. *J Photochem Photobiol A*, 2007, 188: 5–11

# One-step synthesis of fluorescent hydroxyls-coated carbon dots with hydrothermal reaction and its application to optical sensing of metal ions

LIU LiQin<sup>1</sup>, LI YuanFang<sup>1</sup>, ZHAN Lei<sup>2</sup>, LIU Yue<sup>1</sup> & HUANG ChengZhi<sup>1, 2\*</sup>

<sup>1</sup>Education Ministry Key Laboratory on Luminescence and Real-Time Analysis, Ministry of Education; College of Chemistry and Chemical Engineering, Southwest University, Chongqing 400715, China

<sup>2</sup>College of Pharmaceutical Sciences, Southwest University, Chongqing 400715, China

Received April 29, 2011; accepted June 2, 2011

## 1 The optimization of synthesis condition

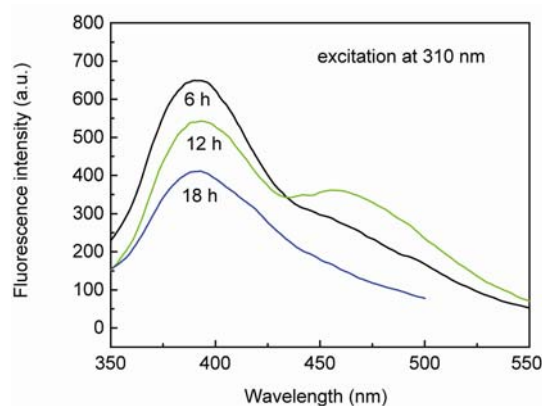


**Figure S1** Fluorescence emission spectra of CDs obtained with different reaction time at 250 °C.

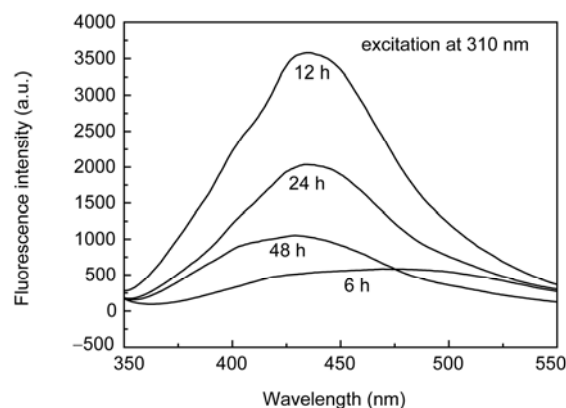


**Figure S2** Fluorescence emission spectra of CDs obtained with different reaction time at 200 °C.

## 2 Quantum yield measurements

Reference on quantum yield (QY) measurements (Lakowicz RJ. *Principles of Fluorescence Spectroscopy* (2nd ed.). New York: Kluwer Academic/Plenum Publisher, 1999, Chapter 8). Quinine sulfate in 0.1 M H<sub>2</sub>SO<sub>4</sub> (literature QY was 0.53 at 310 nm) was served as standard. QY was calculated according to the following classic equation:

$$\varphi_x = \varphi_s \times [A_s/A_x] \times [I_x/I_s] \times [\eta_x/\eta_s]^2$$

Where “ $\varphi$ ” was the QY, “ $I$ ” was the integrated emission intensity, “ $A$ ” was the optical density, “ $\eta$ ” was the refractive index. The subscript “s” and “x” referred to standard reference substance and sample to be determined, respectively. The QY of CDs was 5.5% according to the equation.

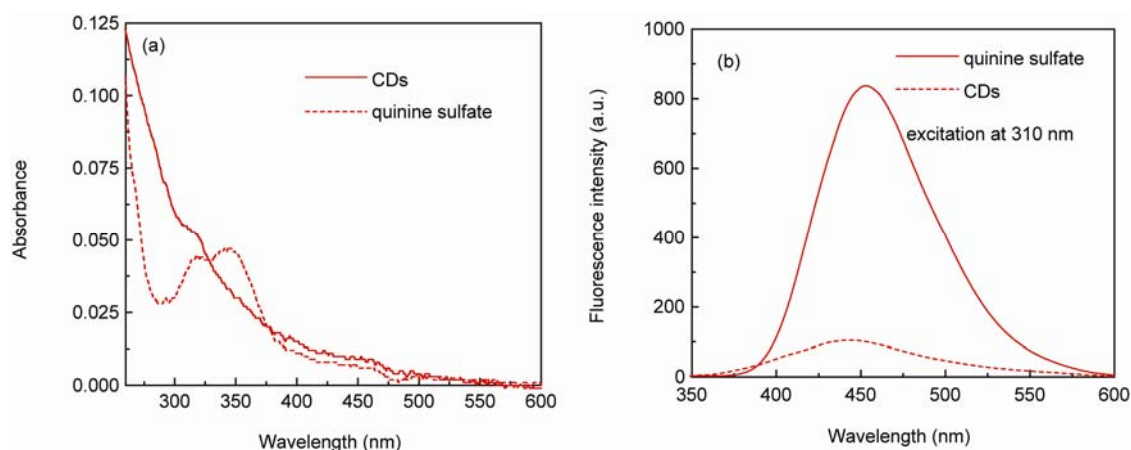


**Figure S3** UV-vis absorption (a) and fluorescence emission spectra (b) of CDs in aqueous solution and quinine sulfate in 0.1 M H<sub>2</sub>SO<sub>4</sub> (CDs obtained with the synthesis condition of 200 °C for 12 h).

**Table S1** Quantum yield of CDs obtained at different conditions in aqueous solution

Sample	Integrated emission intensity ( <i>I</i> ) (390–550 nm)	Abs. at 310 nm ( <i>A</i> )	Refractive index of solvent ( <i>n</i> )	Quantum yield ( <i>φ</i> )
Quinine sulfate	69592.9	0.040	1.33	0.53
CDs (200 °C, 6 h)	3597.0	0.057	1.33	0.019
CDs (200 °C, 12 h)	9899.4	0.055	1.33	<b>0.055</b>
CDs (200 °C, 24 h)	1176.4	0.032	1.33	0.011
CDs (200 °C, 48 h)	657.2	0.078	1.33	0.003
CDs (250 °C, 6 h)	6558.5	0.059	1.33	0.034

### 3 Characterization

#### 3.1 Dynamic light scattering (DLS) and zeta potential

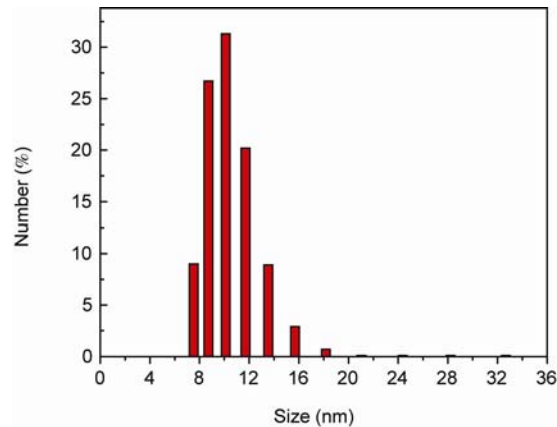


**Figure S4** DLS size distribution of CDs in aqueous solution.

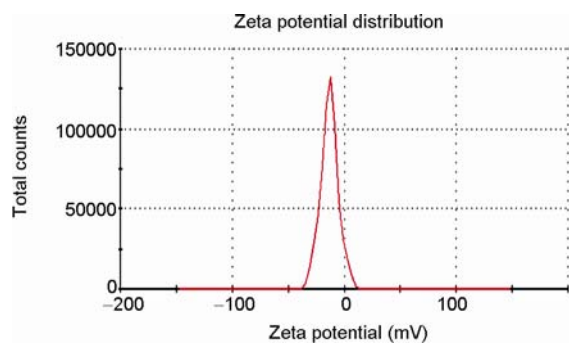


**Figure S5** Zeta potential of CDs in aqueous solution.



### 3.2 Fluorescent emission spectra at different excitation wavelengths

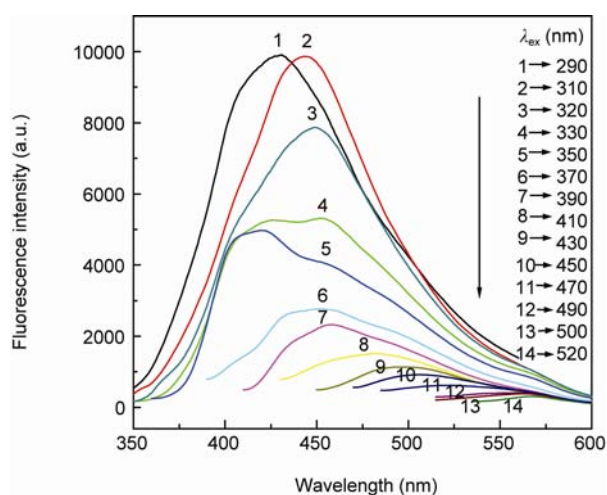


**Figure S6** Fluorescence emission spectra of CDs at different excitation wavelengths as indicated.

### 3.3 Effect of pH

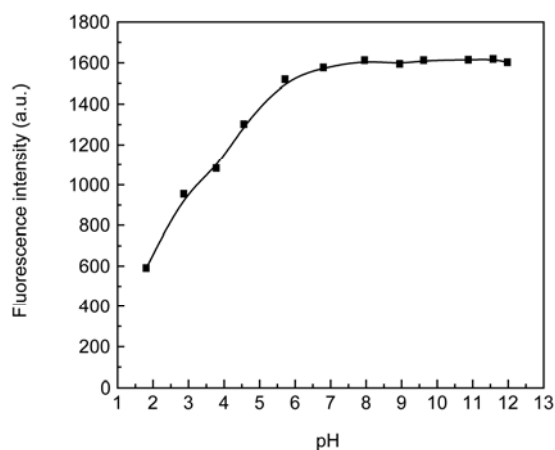


**Figure S7** Fluorescence intensity change of CDs at different pH, buffer: Britton Robinson.

### 3.4 Photostability

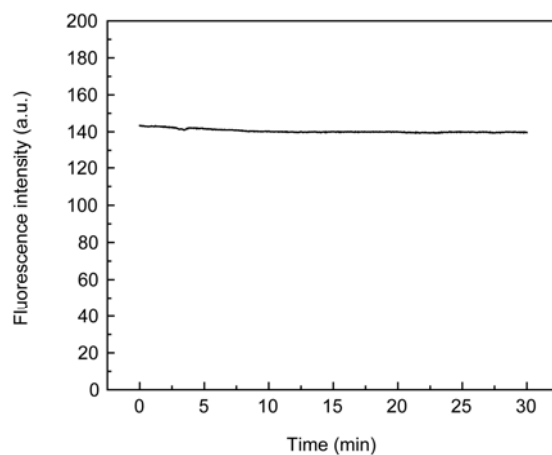


**Figure S8** Effect of the excitation time on the fluorescence intensity of CDs.

### 3.5 Effect of ionic strength

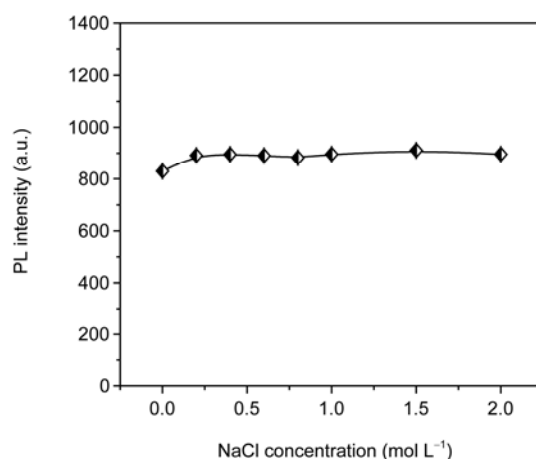


**Figure S9** Effect of the ionic strength on the fluorescence intensity of CDs in NaCl aqueous solution.

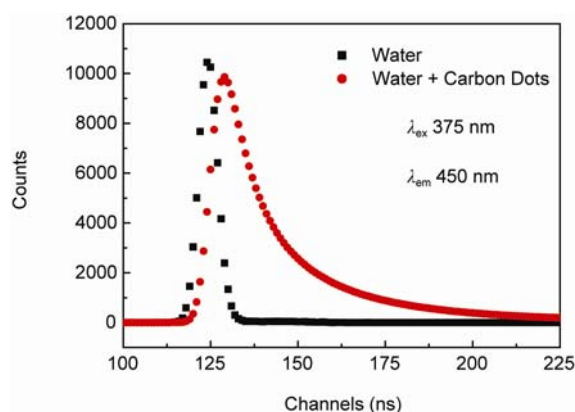
## 4 Cytotoxicity experiment

100  $\mu$ L suspension of Hella cells in Minimal Essential Medium supplemented with 10% fetal bovine serum was added to each well of a 96-well plate. The cells were cultured first for 24 h in an incubator (37 °C, 5% CO<sub>2</sub>), and for another 24 h after the culture medium was replaced with 100  $\mu$ L of MEM containing the CDs at different doses. Then, 10  $\mu$ L of CCK-8 solution was added to every cell well which washed with PBS buffer twice and contained PBS 90  $\mu$ L. The cells were further incubated for 1 h. The optical density (OD) of the mixture was measured at 450 nm with a Microplate Reader Model. The cell viability was estimated according to the following equation:

$$\text{Cell viability [\%]} = (\text{OD treated} / \text{OD control}) \times 100$$

Where OD control was obtained in the absence of CDs, and OD treated obtained in the presence of CDs.

## 5 Fluorescence lifetime



$\tau_i$ (ns)	$A_i$
5.79	54.62 %
1.55	26.52 %
17.37	18.86 %

**Figure S10** Fluorescence lifetime intensity decay of CDs in aqueous solution (average = 6.95 ns).

## 6 Preparation of samples for TEM

Diluted supernatants containing CDs were dropped onto copper grids covered with amorphous carbon film to prepare specimens for transmission electron microscopic observation which were performed in a JEM-2100 microscope with a LaB<sub>6</sub> electron gun operating at 200 kV.